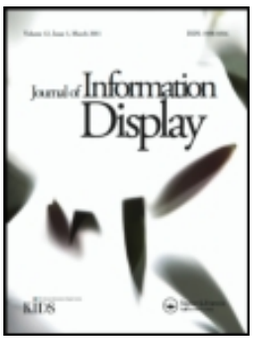

Journal of Information Display

ISSN: 1598-0316 (Print) 2158-1606 (Online) Journal homepage: https://www.tandfonline.com/loi/tjid20

LCD with tunable viewing angle by thermal modulation of optical layer

Jin Seog Gwag , You-Jin Lee , In-Young Han , Chang-Jae Yu & Jae-Hoon Kim

To cite this article: Jin Seog Gwag , You-Jin Lee , In-Young Han , Chang-Jae Yu & Jae-Hoon Kim (2009) LCD with tunable viewing angle by thermal modulation of optical layer, Journal of Information Display, 10:1, 19-23, DOI: 10.1080/15980316.2009.9652074

To link to this article: https://doi.org/10.1080/15980316.2009.9652074

LCD with Tunable Viewing Angle by Thermal Modulation of Optical Layer

Jin Seog Gwag[a], You-Jin Lee[b], In-Young Han[**b], Chang-Jae Yu[*b], and Jae-Hoon Kim[*b]**

Abstract

In this paper, we review the proposed liquid crystal display (LCD) with a tunable viewing angle consisting of a conventional liquid crystal display (LCD) panel and a thermally variable retardation layer (TVRL) characterized by uniformly aligned LC film with transparent indium-tin-oxide electrodes for Joule heating. In the TVRL, nematic phase is transitioned into isotropic by Joule heating. The numerical calculation showed that the intrinsic wide viewing angle was achieved at the isotropic phase of the TVRL by Joule heating, whereas the narrow viewing angle was obtained at the nematic phase of the TVRL. The simulated and experimental results of the proposed LCD show continuous and symmetrical viewing angle characteristics by tuning the retardation of TVRL using Joule heating. The structure of the viewing angle control proposed here is adoptable to all LCD modes with wide viewing angle characteristics.

Keywords : Liquid crystal display, birefringence, viewing angle control

1. Introduction

Various techniques have been developed to improve the viewing characteristics of nematic liquid crystal displays (LCDs), such as patterned vertical alignment (PVA), multi-domain VA (MVA) mode, in-plane switching (IPS) mode, fringe field switching (FFS) mode, and optically compensated bend (OCB) mode [1-8]. Also, as mobile electronic devices become more affordable, the security of privacy has recently become one of the most crucial issues in display functionality. There are instances when the displayed information would be shared with other people and there are instances when the security of such information must be maintained in public places. To meet such needs in a mobile environment, a display with controllable viewing angles is urgently required to enable the user to easily shift between public and private modes: a wide viewing angle (WVA) characteristic for public mode and a narrow viewing angle (NVA) characteristic for private mode. To control the viewing angle, various methods adopting a dual backlight system or two LC panels (side and main panel) have been proposed [9-13]. However, with the dual backlight system, it may be difficult to control the viewing angle continuously because there are only two light paths for NVA and WVA. On the other hand, although the use of two LC panels can exhibit a continuous viewing angle, they cannot have symmetrical viewing angles at intermediate viewing angle ranges due to the one-directional switching of LCs in the side panel that controls the viewing angle. The creation of a symmetrical viewing angle in an intermediate viewing range requires multi-domain LC pixels in the side panel that align well to the pixels of the main panel via a complicated fabrication process. So we hereby propose a simple method of easy control of the LCD's viewing angle [14-17].

In this paper, we review the idea on controlling the viewing angle of an LCD through a thermally variable retardation layer (TVRL) and report on the numerical simulations of the LCD with the TVRL characterized by homeotropic or homogeneously aligned LC cell with transparent indium-tin-oxide (ITO) electrodes for Joule heating. When the TVRL is in isotropic phase by Joule heating, the optical property of the whole LCD is governed only by the main LCD panel and then WVA characteristics is achieved. On the other hand, when TVRL is in the aligned nematic

Manuscript received February 26, 2009; Revised March 9, 2009; accepted for publication March 20, 2009.
This work has been supported by LG display and the Korea Research Foundation Grant funded by the Korean Government (MOEHRD) (KRF-2006-005-J04103).
* Member, KIDS; ** Student Member, KIDS
Corresponding Author : Jae-Hoon Kim
[a] Department of Physics, Yeungnam University, Kyeongsan-si 712-749, Korea
[b] Department of Electronics and Computer Engineering, Hanyang University, Seoul 133-791, Korea
E-mail : jhoon@hanyang.ac.kr **Tel** : 02-2220-0343 **Fax** : 02-2298-0345

phase by cooling or no heating, the optical property of the LCD at the off axis is influenced crucially by TVRL despite the fact that the front side is not influenced, and then NVA is achieved. The simulated and experimental results of the proposed LCD show continuous and symmetrical viewing angle characteristics by tuning the retardation of TVRL using Joule heating. In our structure, the TVRL is attachable to other LCDs and thus wide viewing LCD modes, such as PVA, MVA, IPS, FFS, and OCB modes can be used as the main display panel.

2. Principle and preparation for experiment in FFS mode

Figure 1 shows the schematic diagram of how to obtain WVA and NVA in LCD structure with fringe field switching (FFS) nematic mode combined with the TVRL, which is composed of a homeotropically aligned LC layer between two plastic substrates. Patterned transparent electrodes for Joule heating are formed on one substrate for temperature control. When the TVRL is in the isotropic phase, which does not have any optical anisotropy by heating as shown in Fig. 1(a), the optical characteristics of the LCD will be determined only by the main panel (FFS panel). In this case, when voltage is not applied, the FFS mode, in which the LCs are aligned parallel to the transmissive axis of the light-input polarizer, shows an excellent dark state. This is due to the fact that the input light of 0˚ linear polarization, which passes through the LC layer without changing the polarization, is blocked perfectly by the output polarizer with a 90˚ transmissive axis. The bright state can be achieved when the LC director is rotated ideally by 45˚ by the horizontal field. In this case, the input light of 0˚ linear polarization is rotated about 90˚ at the LC layer. Consequently, the FFS mode connected with TVRL with an optically isotropic state exhibits WVA, an optically high contrast ratio for all viewing directions due to the absence of polarization changes in the light while in the dark state, even when light is obliquely incident. On the other hand, when the non-heating TVRL is in the vertically aligned nematic phase as shown in Fig. 1(b), it does not have any optical anisotropy in the normal incidence of light. Thus, the LCD shows a good image quality in the front view because the TVRL does not have an optical effect on the main panel in the front view. However, the side view with obliquely incident light has an optical influence on the main panel because the vertically aligned LC has optical anisotropy at oblique incident. Consequently, the LCD shows light leakage in the side view of the dark state. This is the reason why the FFS mode connected with TVRL with a vertically aligned nematic phase leads to NVA, an optically high contrast ratio for only the front view. As a result, we will obtain both the WVA and NVA in the LCD by tuning the retardation of the TVRL through well controlled thermal heating.

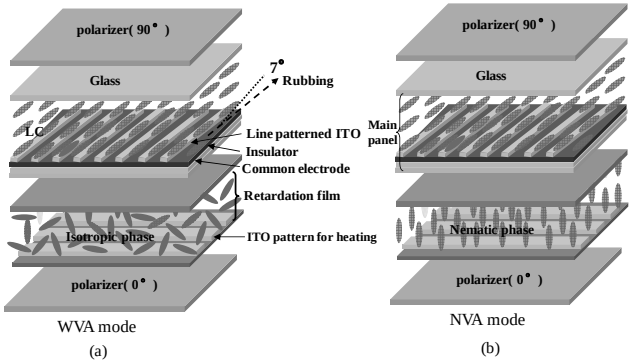

Fig. 1. Schematic diagram of the structure of the proposed LCD with tunable viewing angle: (a) narrow viewing angle using the nematic phase of TVRL; (b) wide viewing angle using the isotropic phase of TVRL

We used AL60702 (JSR) as a homeotropic LC alignment layer of TVRL and SE-7492 (Nissan Chemicals), which yields a pre-tilt angle of 6˚ after general rubbing, as the LC alignment layer of the FFS cell. The width and gap of the interdigitated electrode (line-patterned electrode) of the FFS cell were 4 um and 5 um, respectively. The bottom (common) electrode was separated from the interdigitated electrode by a 200-nm-thick layer of SiNx functioning as an insulator. The electrode material used here was indium-tin oxide. The cell gap of the FFS and the thickness of the TVRL were 3.4 μm and 5.5 μm, respectively. The LCs injected into the FFS cell and TVRL were MAT-03-151 (Merck, Δn=0.104 at 20°C) and E7 (Merck, Δn=0.2249 at 20°C), respectively.

3. Experimental and simulated results in FFS mode

We performed a simulation using a commercial LCD simulator from TechWiz LCD. Figure 2 (a) shows continuous viewing angle characteristics that depend on the temperature-dependent birefringence of TVRL. In the simulation, we set the cell gap and birefringence of the FFS cell to

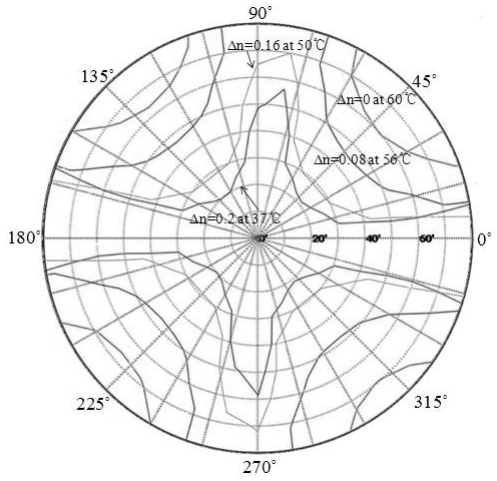

(a)

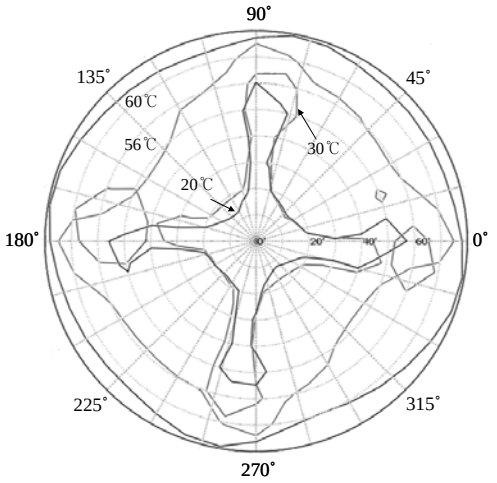

(b)

Fig. 2. Viewing angle characteristics: (a) simulated results of viewing angle depending on the birefringence of TVRL determined by temperature in the proposed viewing angle controllable FFS mode, (b) measured results of viewing angle according to the temperature of TVRL in the proposed viewing angle controllable FFS mode.

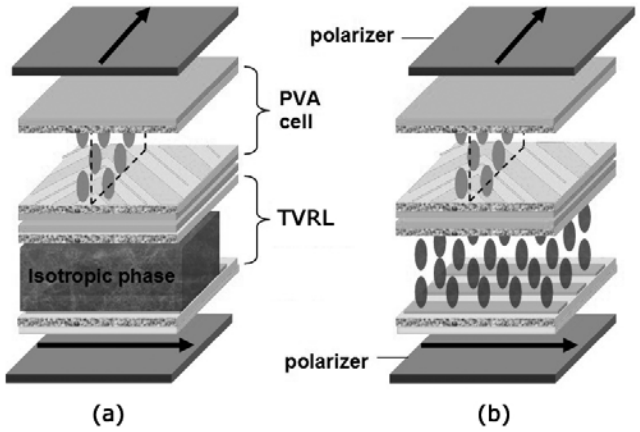

Fig. 3. The cell structure of a viewing angle controllable LCD. (a) WVA mode in the thermally activated state (isotropic phase) and (b) NVA mode in the normally homeotropic state (isotropic phase) of the TVRL.

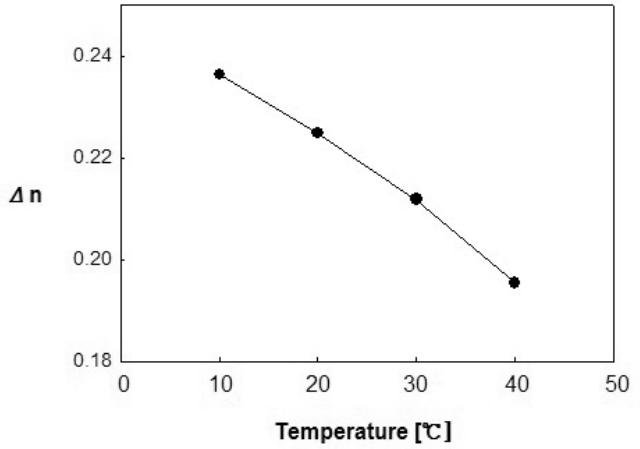

Fig. 4. The refractive anisotropy of E7 as a function of temperature

3.6 μm and 0.1, respectively. The thickness of TVRL was 5.5 μm. As expected, the simulation results demonstrate a symmetrical viewing angle as well as a continuous viewing angle change with the changing birefringence of the TVRL, which is controlled by temperature. Figure 2 (b) shows the experimental results of viewing angle characteristics of the FFS LCD with the different temperatures of E7-TVRL. The viewing angle was measured by DMS-900 (Autronic Melchers Co.). As shown in Fig. 4, we can obtain a contrast ratio (CR) greater than 10:1 from almost all viewing areas in the contours with polar angle limits of 80˚ with TVRL in an isotropic phase (60°C). The WVA characteristics came from the properties of FFS. If we decreased the temperature of TVRL in the nematic phase (20°C), CR values greater than 10:1 are limited to 20˚ in the diagonal direction. We can control viewing angle characteristics for intermediate viewing angle ranges by adjusting the temperature between 20°C and 58°C. Moreover, the viewing angle characteristics are symmetrical in all viewing angle ranges.

4. Simulated result in PVA mode

As another approach, we examine the viewing angle controllable PVA mode through optical simulation. The structure of the LCD with controllable viewing angle pro-

posed here is shown in Fig. 3. The birefringence of Δ*nd* in the TVRL plays an important role in the viewing angle characteristics of the whole LCD with the TVRL. As previously mentioned, because the optical property of the viewing angle controllable LCD is governed by that of the main LCD panel for the isotropic phase through heating the TVRL as shown in Fig. 3(a), the widest viewing angle is obtained in the conventional PVA mode without the TVRL. At the normally homeotropic state of the TVRL, the wide viewing angle characteristics would be degraded due to the strong dependence of the birefringence on the polar angle as shown in Fig. 3(b).

In general, the LC materials for the TVRL possess as low nematic-isotropic transition temperature (T_{NI}) as in the vicinity of room temperature to reduce the power consumption by Joule heating and heating effect on the main LCD panel. For simulation, we used the material parameters of E7 (E. Merck), as the LC in TVRL, of which T_{NI} is about 58°C. To calculate the viewing angle of a PVA LC mode with TVRL, a commercial simulator of TechWiz LCD (Sanayi System Co., Ltd., Korea) was used. For simulation, the refractive anisotropy of the VA LC material and the cell thickness were used to be 0.0824 and 4.36 μm in the conventional PVA mode, respectively. Here, an operating voltage of the PVA mode was used to be 7.5 V.

The refractive anisotropy of E7 for the TVRL is 0.2255 at room temperature and its temperature dependence is shown in Fig. 4. It should be noted that the optical properties are governed by the birefringence of the TVRL. As shown in Fig. 4, the refractive anisotropy of the E7 for the TVRL gradually decreases and reaches zero above the T_{NI} with the increasing temperature and thus the viewing angle characteristics of the PVA LC mode with the TVRL are continuously controlled within a certain range. For simplification of the simulation, we fixed the cell thickness (*d*) of the heating layer, TVRL, and changed the refractive anisotropy (Δ*n*) from 0 to 0.2255. It should be noted that the refractive anisotropy even in the homeotropically aligned structure still depends on temperature.

The viewing angle characteristics of the PVA LC modes with the TVRL simulated here are shown in Fig. 5. In the isotropic phase of the TVRL produced by Joule heating, the intrinsic viewing characteristics of the PVA LC mode were obtained as shown in Fig. 5(a). In such case, the effect of the TVRL is negligible due to the independence of incident direction and polarization in the isotropic phase of the

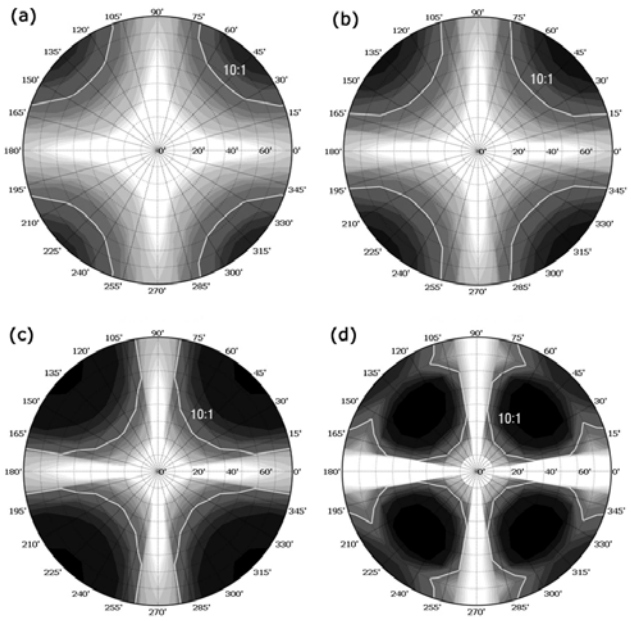

Fig. 5. The contours of the contrast ratios of the PVA LC mode with the TVRL for various retardations (Δ*nd*) of the TVRL. (a) Δ*nd* = 0.0, (b) 1.0, (c) 1.7, and (d) 2.2. The solid lines in each contour represent the boundaries of the contrast ratio 10:1.

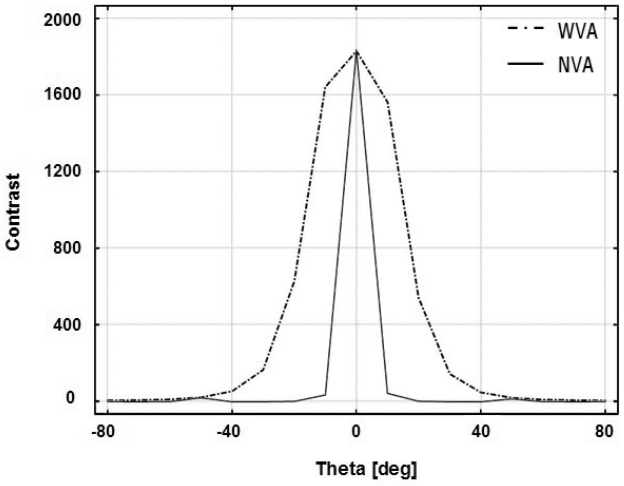

Fig. 6. The contrast ratios of the WVA (Δ*nd* = 0.0) and NVA (Δ*nd* = 2.2) modes along the diagonal axis.

TVRL. Here, an excellent contrast ratio was achieved within a range of our simulations (WVA mode).

In principle, the contrast ratios are gradually reduced with the increase in the birefringence of the TVRL within a range of our simulation because of the enhancement of the birefringence dependence on the polar angle as shown in Fig. 5. In the NVA mode with the birefringence of Δ*nd* =

2.2, the polar angle with the contrast ratio 10:1 was decreased up to 20° along the diagonal axis as shown in Fig. 5(d). Here, LC molecules in the TVRL shows a nematic phase and is uniformly aligned by the alignment layer. In the homeotropically aligned structure, note that the refractive anisotropy at a normal incidence does not have an effect on the contrast ratio but that at any oblique incidence produce the degradation of the contrast ratio. Therefore, the viewing angle characteristics could be controlled by the heating layer of the homeotropically aligned LC structure.

Figure 6 shows the contrast ratios of the WVA mode, where the LC in the TVRL transitions isotropic phase by Joule heating, and the NVA mode at the nematic phase with Δnd = 2.2 along the diagonal axis. It is obvious that the viewing angle is remarkably reduced by the TVRL with a nematic phase.

5. Conclusions

We reviewed our continuous viewing angle controllable LCD with the use of a temperature-dependent retardation film. By changing the birefringence of the film with Joule heating, the viewing angle of the FFS LCD can be controlled continuously. From the numerical simulations of the PVA LC cell with the TVRL, the WVA mode was obtained by Joule heating in the TVRL where the LC molecules transitioned into isotropic phase and thus no influence occurred on the viewing angle characteristics. On the other hand, the NVA mode was achieved at the nematic phase in the TVRL. Therefore, we believe that the proposed LC display is suitable for mobile phones, notebook computers, and E-book readers with viewing angle controllable function.

References

[1] T. Miyashita, Y. Yamaguchi, and T. Uchida, Jpn. J. Appl. Phys., **34**, L177, (1995).

[2] K. H. Kim, K. Lee, S. B Park, J. K. Song, S. N. Kim, and J. H. Souk, The 18th International Display Research Conference Asia Display '98, p. 383.

[3] M. Oh-e and K. Kondo, Appl. Phys. Lett., **67**, 3895, (1995).

[4] S. H. Lee, S. L. Lee, and H. Y. Kim, Appl. Phys. Lett., **73**, 2881, (1998).

[5] J. S. Gwag, K.-H. Park, J. L. Lee, J. C. Kim, and T.-H. Yoon, Jpn. J. Appl. Phys., **44**, 1875, (2005).

[6] J. S. Gwag, J. Fukuda, M. Yoneya, and H. Yokoyama, Appl. Phys. Lett., **91**, 073504, (2007).

[7] J. S. Gwag, J.-H. Kim, M. Yoneya, and H. Yokoyama, Appl. Phys. Lett., **92**, 153110, (2008).

[8] J. S. Gwag, K. Shon, Y.-K. Kim, and J.-H. Kim, Opt. Exp., 16, Accepted (2008).

[9] K.-W. Chien, Y. –J. Hsu, and H.-M. Chen, SID Int, Symp. Digest Tech. Papers **37**, 1425 (2006).

[10] K. Takatoh, S. Kobayashi, S. Kimura, N. Okada, T. Kanetsuna, N. Hirama, S. Kurogi, S. Sekiguchi, and K. Uemura, SID Int, Symp. Digest Tech. Papers **37**, 1340 (2006).

[11] M. Adachi and M. Shimura, SID Int, Symp. Digest Tech. Papers **37**, 705 (2006).

[12] J.-I. Baek, Y.-H. Kwon, J. C. Kim, and T. H. Yoon, Appl. Phys. Lett. **90**, 101104 (2006).

[13] E. Jeong, Y. J. Lim, J. M. Rhee, S. H. Lee, G..-D. Lee, K. H. Park. and H. C. Choi, Appl. Phys. Lett. **90**, 051116 (2007).

[14] J. S. Gwag, Y.-J. Lee, M.-E. Kim, J.-H. Kim, J. C. Kim, and T.-H. Yoon, Opt. Express **16**, 2663-2668 (2008).

[15] In Young Han, Jin Seog Gwag, You Jin Lee and Jae-Hoon Kim, IMID08, 348 (2008).

[16] Jin Seog Gwag, In-Young Han, Chang-Jae Yu, Hyun Chul Choi, and Jae-Hoon Kim, Opt. Express (Accepted).

[17] In Young Han, Jin Seog Gwag, You Jin Lee, Chang-Jae Yu, and Jae-Hoon Kim, Mol. Crys. Liq. Crys., (Accepted).

※ Parts of this work were presented in Proceedings of IMID 2008.